Petroleum Res. J. Vol. 21 (2008/2009); P. 81–98, 14 Figs.

Petrography, Diagenetic Aspects and Isotopes of the An Nagaza Member of the Al Khums Formation, NW Libya

Mahmoud T. Elbakai*, Aisha, K. Shalghum* and Lila I. Hafez*

Abstract: Petrographic, and geochemical analyses were carried out on a total of 33 samples from the An Nagaza Member of the Al Khums Formation in NW Libya. The An Nagaza sediments have been divided into five lithofacies. These lithofacies are mainly of grainsupported and they started with sediments resulted from transgression over a Cretaceous and/or Triassic surface of moderate relief. Various fossils and abundance of silisiclastic materials suggest a shallow marine environment. The complete succession of the An Nagaza sediments is interpreted as a transgressive sequence over the Cenomanian succession, passing from marginal marine possibly to fully marine deposits. Several diagenetic events took place during deposition of the sediments of the An Nagaza Member in a different diagenetic environments. These events include micritization, cementation, compaction and dissolution. These diagenetic processes occurred in marine phreatic zone, mixed marine and meteoric zone, meteoric zone and shallow burial environment. Low concentration of Sr and Mn of the An Nagaza samples could be attributed to the diagenetic effects produced by meteoric solutions. High concentration of Fe in the An Nagaza samples suggest that all samples are not exclusively carbonate and contain appreciable amounts of clay minerals and quartz grains. Depleted or negative values of $\delta^{18}O$ in the An Nagaza samples probably indicate the influence of sea-level fluctuation during Miocene, influx of meteoric water and recrystallization of early carbonate cements. Furthermore, changes of $\delta^{13}C$ from low values in the bottom to relatively higher values and return to a low $\delta^{13}C$ values in top of the sequence may indicate a move from restricted basin with high productivity to more marine conditions and back again. Analysis of Sr isotopes suggest that an Early Miocene age is postulated for the An Nagaza Member of the Al Khums Formation.

Keywords: Al Khums Formation, An Nagaza, marine phreatic, meteoric, $\delta^{13}C$, $\delta^{18}O$.

INTRODUCTION

The succession of the exposed outcrop unites in northwestern Libya (Fig 1) ranges from Triassic to Late Miocene (Fig. 2).

Al Khums Formation is the only record of the Tertiary in this area, although Tertiary strata occur both to the southwest and to the east, in the Sirt Basin (Barr and Weegar, 1972). Al Khums Formation consists chiefly of a limestone, chalk and marly limestone interbedded with thin layers of sandy limestone and clay, much of it contains both mega fossils and microfossils. Al Khums Formation has been divided by Salem and Spreng (1980) into two members named the lower An Naggazah member (the target of this study), and upper Ras El Manubyah Member.

The thickness of An Naggazah Member in the study area is approximately 95m, and unconformably overlies Mesozoic rocks. An Naggazah Member can be divided into two units (Salem and Spreng, 1980); the lower Unit (1) consists predominantly of bioclastic, biostormal, and biohermal limestone. This unit was deposited in low areas on eroded Mesozoic rocks, so its thickness is variable and is controlled by the topography of pre-Miocene. Unit (2) is brownish, yellow, marlstone, argillaceous limestone and sandy to silty detrital limestone. Both interbedded with green gypseferous clay beds.

The most common fossils are pectins, high spiral gastropods, oysters, corals, bryozoans, algae and echinoids. (Fig. 3a and b).

Previous Work

Many works have been done on Al Khums

* Libyan Petroleum Institute (LPI), P. O. Box 6431, Tripoli, Libya

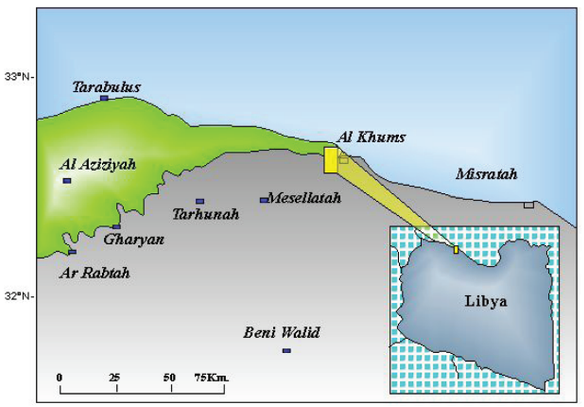

Fig. 1. Location map of Al Khums area.

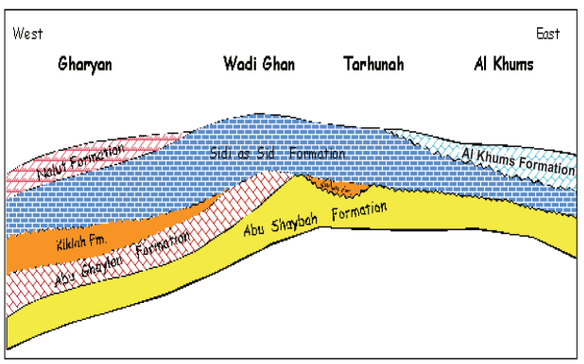

Fig. 2. East-west cross-section through Gharyan Al Khums area (after Fatmi and Sbeta, 1991).

Formation, but most of them concentrated on a stratigraphy and age determination.

The sediments of Al Khums were first distinguished as Middle Miocene. Floridia (1939) and Mann (1975) have introduced the term of Al Khums on the Mediterranean Coast in Tripoli and suggesting a Middle Miocene age during the regional mapping of Libya (1975 to 1984) for IRC.

Zivanovich (1977) added more details on the lower and upper part of Al Khums Formation exposed in Bani Walid and Al Qaddahyah sheets.

Mijalkovic (1977), established the persistence of Al Khums Formation from Al Khums area eastwards as far as An Nawfliya, and all of them attributed it to a Middle Miocene age. The formation was studied and subsequently divided by Salem and Spreng (1980) into two members, a lower An Naggazah Member and an upper Ras Al Mannubya Member. Innocenti and Pertusati (1984) studied the sediments of the formation and determined their age as Late Miocene. El Waer (1988 and 1991) had studied the ostracoda in this area and agreed with the others about the Middle Miocene age. Sherif (1991) determined the same age in his study of the area.

MATERIALS AND METHODS

Several fieldtrips were carried out to the study area in order to measure and log the An Nagaza Member section. A total of 33 samples from 95 meter exposure of this member were collected.

All samples were used for thin-section preparation, subsequently all samples were grinded for atomic absorption analysis in the Libyan Petroleum Institute laboratories and stables isotopes contents in the NERC Isotope Geosciences Laboratory, UK.

Two additional unconsolidated sandstone samples were sieve analyzed in order to help identification of the environment of deposition of this member. All thin-sections were stained according to Dickson's (1965) technique.

The powder of these samples was reacted with anhydrous phosphoric acid in *vacuo* overnight at a constant temperature of 25°C. The CO_2 liberated was separated from water vapour and collected for analysis in the NERC Isotope Geosciences Laboratory, UK. Measurements were made on a VG SIRA mass spectrometer. Overall analytical reproducibility for these samples and standard materials was better than 0.1% for both $\delta^{13}C$ and $\delta^{18}O$ (2σ). Isotope values ($\delta^{13}C$, $\delta^{18}O$) are reported as per mil (‰) deviations of the isotopic ratios ($^{13}C/^{12}C$, $^{18}O/^{16}O$) on the VPDB scale.

150 milligrams of powder were leached overnight with 3mls of IN Romil® ultrapure acetic acid in order to dissolve only the carbonate fraction. Each sample was centrifuged and the supernatant liquid pipetted into a Savillex® FEP beaker and reduced to dryness. The residue was converted to chloride with 1μL double quartz-distilled 6N hydrochloric acid, evaporated until dry and then dissolved in 200 μL of 2.5N HCL. After centrifuging, 100μL of each sample was located onto a standard Biorad® AG50-X8 cation exchange column and eluted in 2.5N HCL. Strontium was loaded on a single tantalum filament with phosphoric acid. Isotope ratios were measured on a Finnegan Triton mass spectrometer run in static mode with mass fractionation normalized to a $^{87}Sr/^{86}Sr$ ratio of 0.1194. At least 170 ratios were collected which resulted in a 'within run' precision of better than 7 x 10^{-6} (2σ). Each sample was analysed twice and the mean of the data is used in this study. Replicate analysis (n = 25) of the international strontium isotope standard NBS-987 yielded a mean value of 0.7102446 ± 0.0000012 (2σ). 16 determinations of the North Atlantic Seawater standard yield a mean $^{87}Sr/^{86}Sr$ ratio of 0.7091689 ± 0.0000091 (2σ).

PETROGRAPHY

The vertical variation in lithology of An Nagaza Member of the Al Khums Formation can be divided into various lithological units or lithofacies started with sediments resulted from transgression onto a Cretaceous surface of moderate relief. Generally, these sediments are of fossiliferous, reef-bearing with basal sand and limestone (Salem and Spreng, 1980). Five lithofacies can be distinguished on bases of field observation; faunal diversity and petrographic analysis (see also Fig. 12). These lithofacies in ascending order are as following:

Lithofacies 1: This lithofacies overlying Cretaceous sediments of Ain Tobi Member of the Sidi as Said Formation and is characterized by transgressive sandstone at its base (Fig. 3c and d). Lithofacies 1 exhibits 13 metres of yellowish, highly fossiliferous (gastropods, bivalves, echinoderms, foraminifera and algae) and irregularly to horizontally bedding marly limestone. The lower 2m of Lithofacies 1 are mainly sandstones composed of quartz grains scattered and float in fine micrite matrix (Fig. 4a and b).

Quartz grains are fine to medium-grained, well rounded to subrounded, rarely subangular, calcareous and unicrystalline. This sandstone containing scattered fossils including (plecypods, foraminifera, echinoderms, corals and gastropods, Fig. 4c). The sand is conglomerate in places, containing flat pebbles and cobbles of limestone. The main non-skeletal allochems occurred in Lithofacies 1 are ooids and pellets (Fig. 4b). They are observed only in the lower part. Ooids are of different size or poorly sorted (very fine to medium) with relatively thin cortices coating detrital quartz nuclei. The early ooids laminae fill in depression on the surface of quartz grains and are absent from angular corners. Ooids with no nucleus seem to be partially and/or completely micritized to form pellets. The skeletal allochems of Lithofacies 1 consist also of large single crystals of echinoderm with early syntaxial calcite overgrowth cement (Figs. 4d and 5a). Small transverse cross-sections of echinoderm spins showing single calcite crystal structure are also observed and scattered within micrite matrix (Fig. 5b). Large fragments of red coralline algae are also present, some of them are well preserved (Fig. 5c) with very thin micrite walls separating small cells and others are fractured.

Both uniserial and biserial and various shapes of miliolid foraminifera are observed within sediments of Lithofacies 1 and are surrounded by micrite envelopes and their typical chambers are filled by sparry calcite (Figs. 5d and 6a). Poorly preserved pryozoa fragments are scattered throughout the

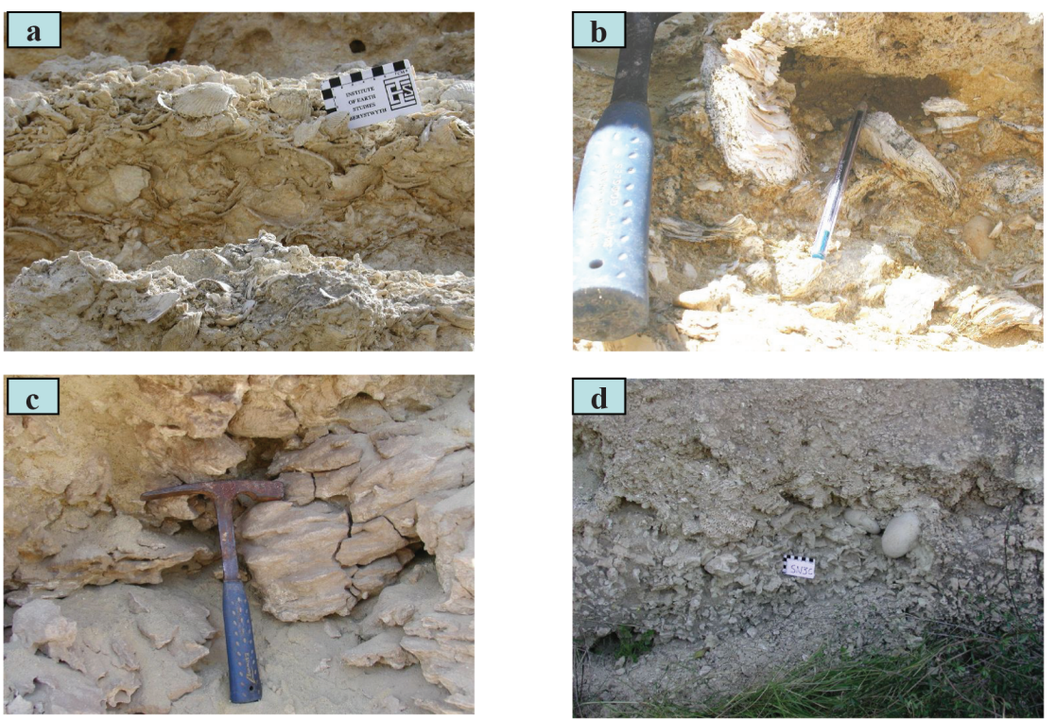

Fig. 3. Field views showing common fossils in An Nagaza sediments (a and b) and the basal sandstone and conglomerate of the An Nagaza Member (c and d)

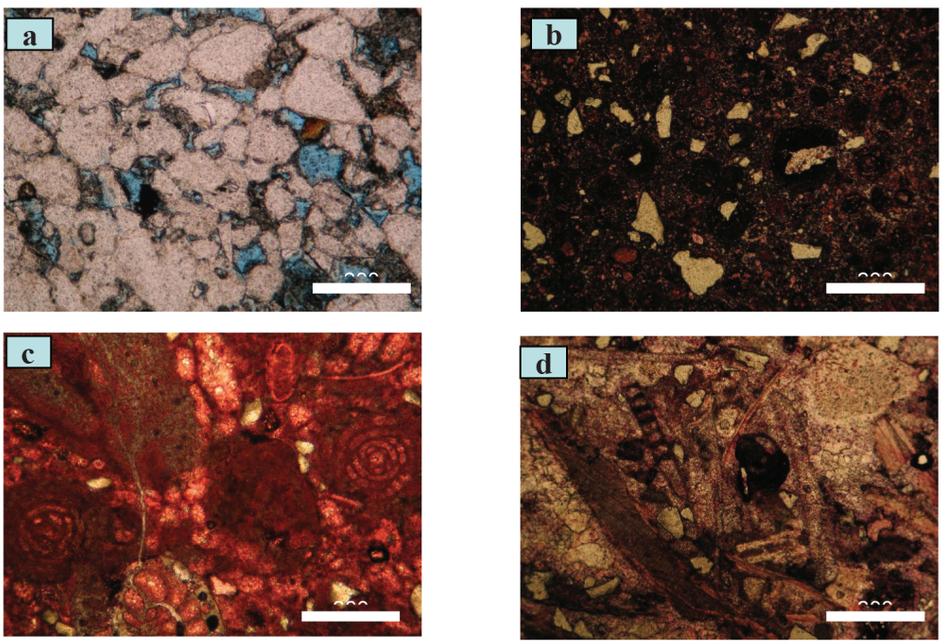

Fig. 4 Microphotographs from An Nagaza Member of the Al Khums Formation. a) Microphotograph showing quartz grains. b) Microphotograph showing ooids within micrite matrix. c) Microphotograph showing different types of foraminifera. d) Microphotograph of uniserial forams and echinoderm plates with syntaxial overgrowth cement.

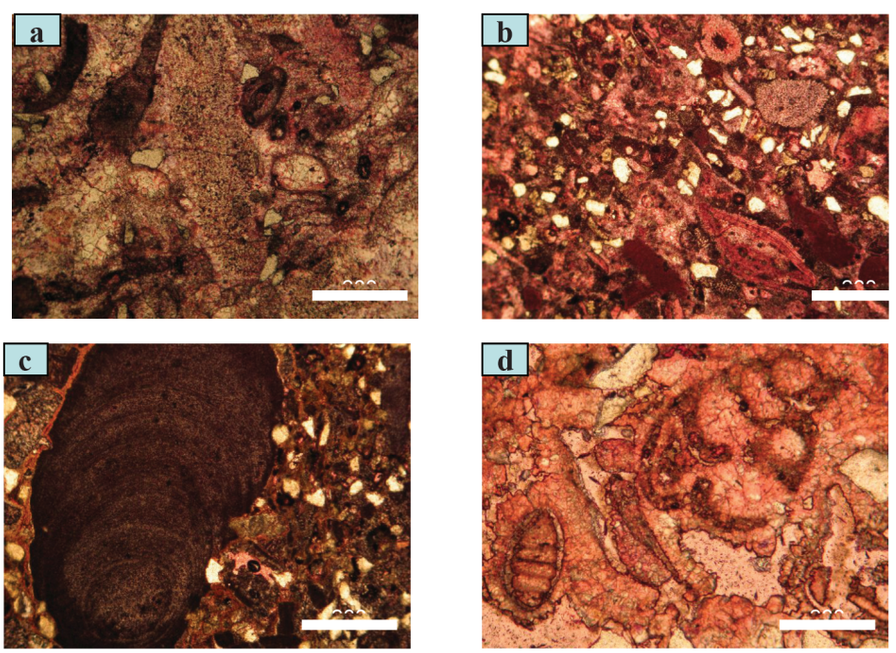

Fig. 5. Microphotographs of An Nagaza Member of the Al Khums Formation: a) Microphotograph of echinoderm plates with syntaxial overgrowth cement. b) Microphotograph showing plates of echinodem and numulites. c) Microphotograph showing good preserved coraline algae. d) Microphotograph of gastropoda shells with micrite envelope. Note also interparticle porosity.

upper part of this lithofacies. Rare transverse sections of brachiopod spins with thick foliated walls (Fig. 6b) are also occurred. No visible porosity observed in most of these sediments.

Sediments of this lithofacies exposed to many diagenetic events; such as cementation and micritization. Lithofacies 1 can be classified as bioclastic wackestone dominated by sandstone at the lower part.

Lithofacies 2: This lithofacies composed of 20 meter of yellowish-grey, irregularly to massively bedded and hard limestone. Sediments of Lithofacies 2 consist of algae, corals, and plecypods, these

organic accumulations thicken locally to form biohermal structure (Salem and Spreng, 1980). Corals are concentrated in the lower part of the lithofacies (Fig. 6c), while echinoderms, bryozoans and plecypods locally form coquinal masses in the upper part. The most common skeletal particles are small, longitudinal and not very well preserved red algae (Fig. 6d). Different sizes of mainly rounded and well preserved echinoderm plates and cross-sections of crinoid spins are also common (Fig. 7a). All cemented by calcite, mainly of syntaxial overgrowth type.

Bryozoa fragments are observed in Lithofacies 2, their cells are separated by thin walls of micrite. These cells are mainly filled by drusy mosaic calcite cement. Some of the bryozoan fragments are influenced by pressure solution event. Cells of bryozoans are similar in the shape to the bees cells (Fig. 7b). Corals are relatively unaltered and illustrating high initial intragranular pore spaces. Some of these pores are filled by sparite.

Miliolids, Numulites (Fig. 7c), fusulinds and biserial forams are rarely observed within sediments of Lithofacies 2. They are mainly characterized by thick micrite walls and their chambers are filled by different texture of calcite.

Quartz grains are the only non-carbonate constituents observed in Lithofacies 2. They are fine, moderately sorted and subrounded unicrystalline grains scattered throughout matrix. Lithofacies 2 can be classified as packstone, becoming grainstone at the top.

Lithofacies 3: This lithofacies begins with sandy limestone. Sand grains are mainly composed of fine, subrounded to subangular quartz grains, scattered throughout the whole lithofacies. The thickness of Lithofacies 3 is 27 metres and it is characterized by very common echinoderms. These echinoid plates are still with their original structure and well preserved spins are also occurred (Figs. 7d and 8a), some of them have syntaxial calcite overgrowth cement.

Rare uniserial and biserial forams are observed in Lithofacies 3. Algae are not common (some of them are completely micritized) and bryozoa cross-sections exhibit fenestral structure, whereas large and very common bryozoan fragments have thick fibrous walls (similar to brachiopod structure) and shows honey-comb structure-like (Fig. 8b). All cells are filled with drusy mosaic cement. Gastropods occur as transversal or longitudinal section within Lithofacies 3. Their chambers are filled by either drusy cement or micrite and outlined by thin micrite envelopes (Fig. 8c). In the upper part of this lithofacies, large fragments of corals composed of typical rounded chambers are common. Some of these chambers are filled by micrite and their outlines are sparite, whereas others are filled by sparite with micrite envelopes outlining them. Rare valves of ostracoda enclosed drusy calcite cement are also observed in the upper

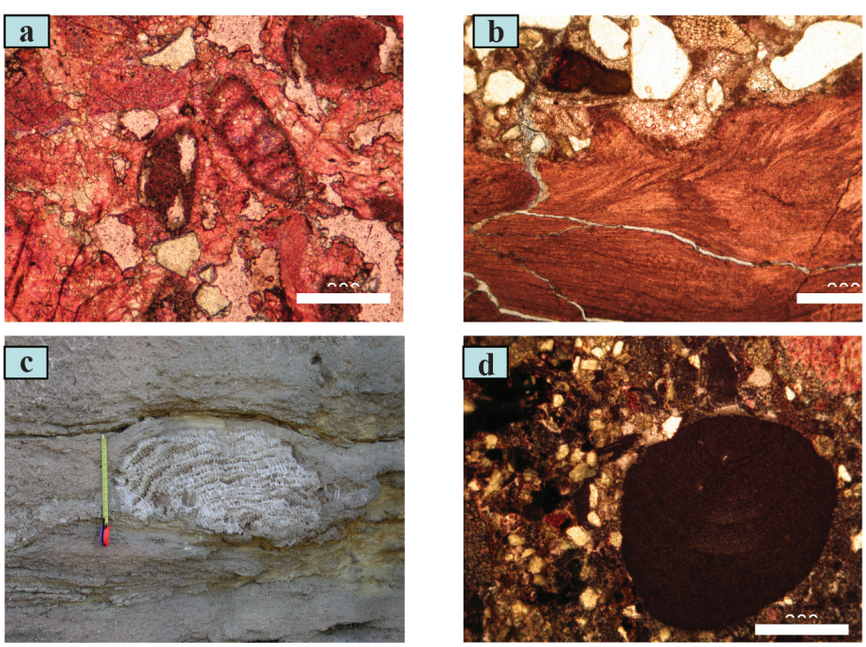

Fig. 6. Microphotographs of An Nagaza Member of the Al Khums Formation: a) Microphotograph of gastropoda shells with micrite envelope. b) Microphotograph showing foliated mollusk fragments. c) Field view of a large corals. d) Microphotograph of well preserved coraline algae.

part of this lithofacies. Sediments of Lithofacies 3 can be classified as biomicrite sandy packstone.

Lithofacies 4: The 16 meter thick sediments of this lithofacies are characterized by brownish-yellow marlstone, argillaceous limestone, and sandy to silty detrital limestone, interbedded with green, gypsiferous clay beds. Lithofacies 4 is the most fossiliferous beds in the entire Al Khums Formation. The common fossils are pectons (Fig. 8d), highly spired gastropods, corals, echinoderms (Fig. 9a) and shallow marine foraminifera. Corals of Lithofacies 4 represented by large fragments exhibit very thick walls with wavy micrite laminae and various chamber sizes. Chambers are outlined by micrite envelopes and mainly filled by drusy calcite cement. Longitudinal

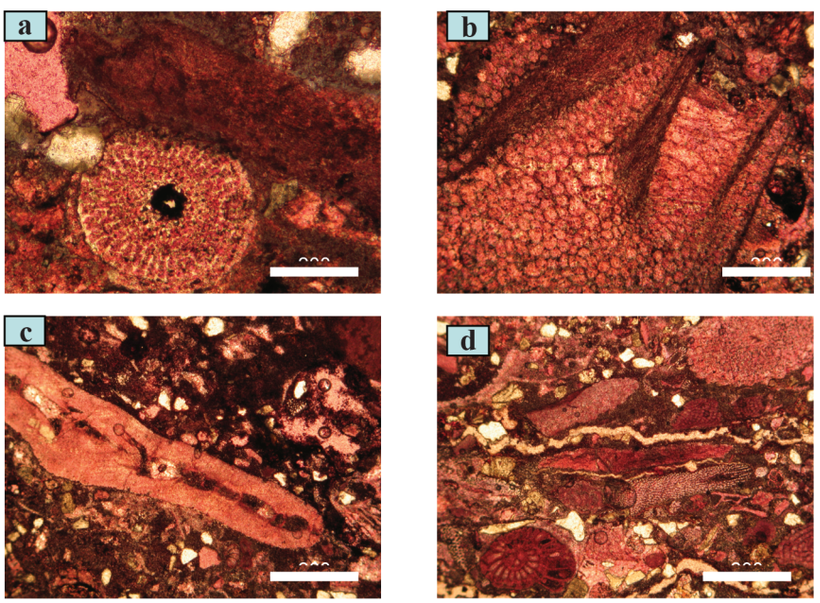

Fig. 7. Microphotographs of An Nagaza Member of the Al Khums Formation: a) Microphotograph showing echinoderm plates and may show influence of compaction on particle grains. b) Microphotograph showing typical structure of bryozoan fragment. c) Microphotograph showing well preserved foraminifera. d) Microphotograph of echinoderm plates and foraminifera + quartz grains. Note the fracture caused by physical compaction.

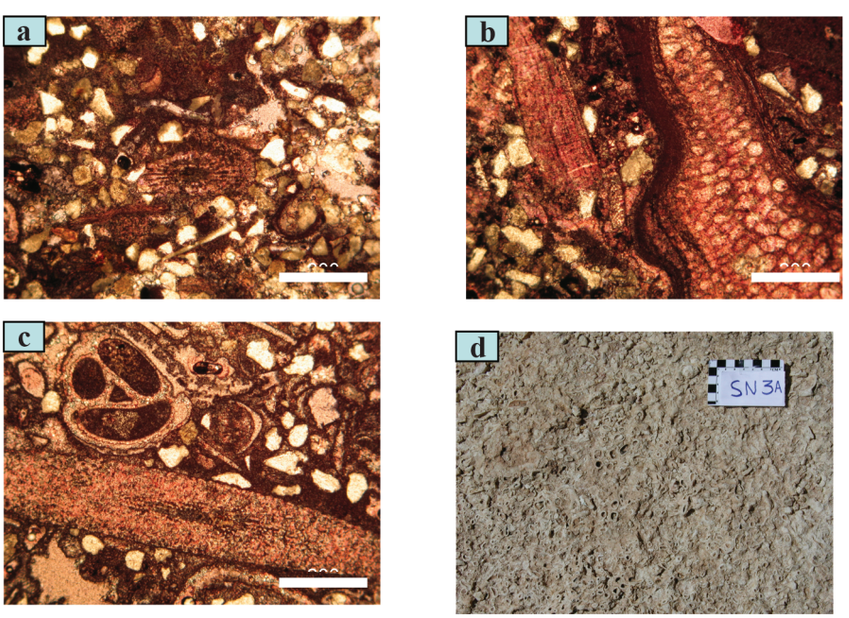

Fig. 8. Microphotographs of An Nagaza Member of the Al Khums Formation: a) Microphotograph showing echinoderm spins (in the centre of photo) with common quartz grains. b) Microphotograph showing typical structure of bryozoan fragment. c) Microphotograph showing well preserved echinoderm spins and transverse section of gastropoda. d) field view showing highly fossiliferous layer.

plates of echinoderm are not common and composed of single calcite crystal; some of them are well preserved.

Transverse section of highly spired gastropods also occurred. They are replaced by non-ferroan calcite. Common, shallow marine uniserial forams are observed at the uppermost part of Lithofacies 4. Forams are outlined by micrite envelopes and filled by recrystallized calcite cement. Sediments of Lithofacies 4 are dominated by bioclastic sandy packstone/grainstone.

Lithofacies 5: The 20 meter thick limestone of this lithofacies may represent shallower marine sediments compared with Lithofacies 4. Lithofacies 5 consists of cross section of bryozoans, with drusy mosaic cement filling chambers. Rare uniserial, biserial and miliolid forams are also observed. Very well preserved longitudinal and rounded plates of echinoderm occurred within the whole lithofacies and exhibit syntaxial calcite overgrowth cement (Fig. 9b). Very common large fragments of corals occur and showing thick wavy micrite walls.

The non-skeletal particles occurred in this facies are ooids. They are rounded and poorly sorted, some of them are enclosed single and foliated crystal of calcite (probably of coral fragments) or quartz grain (Fig. 9c), whereas others are partially or completely micritized. Sediments of Lithofacies 5 can be correlated (on bases of constituents) with those of Lithofacies 1. The top of this lithofacies is dominated by marly limestone with very common algae and branched bryozoans (Fig. 9d). Quartz grains of Lithofacies 5 are moderately sorted, rounded to sub-rounded and unicrystalline. This lithofacies can be classified as biomicrite sandy wackestone/packstone.

DIAGENESIS

The sediments of the Al Khums Formation, particularly the An Nagaza Member) were exposed to several different diagenetic processes. These lead to modification of their original textural and compositional characteristics.

Micritization

Here, blue green algae bore into skeletal material in the shallow marine environment. The borings, re filled with micrite after death of the algae. This process continued and the margin of a shell fragment may become completely replaced by micrite (Fig. 4c) to form micrite envelope (Adams *et al*, 1984, Bathurst, 1975). Micrite envelopes developed on possibly brachiopod (Fig. 9c), brayozoa shells (Fig. 8b) and foraminifera (Figs. 5d and 6a).

Repeated formation of micrite envelopes, may lead to the production of a grain completely micritized with no remaining recognizable structure.

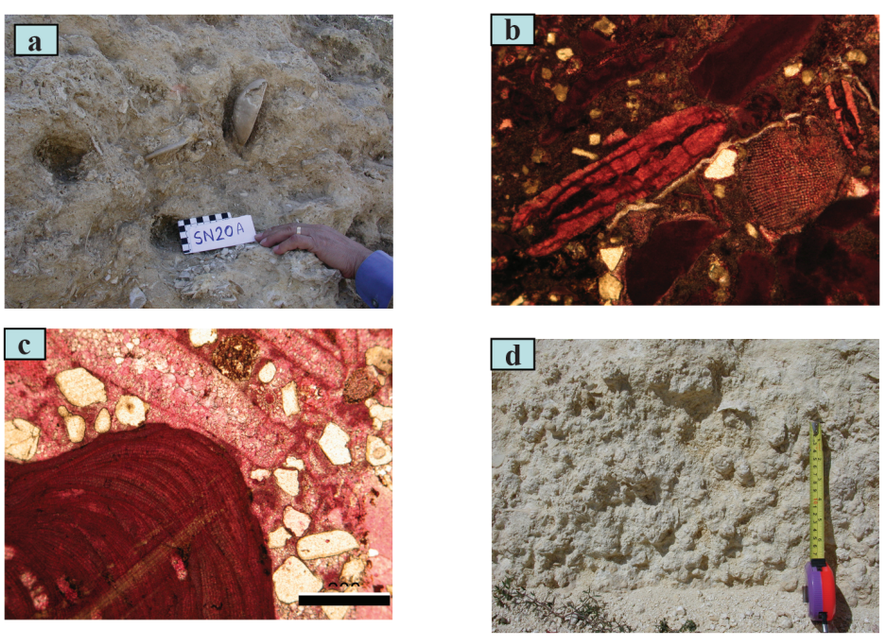

Fig. 9. Field view and microphotograph of An Nagaza Member of the Al Khums Formation: a) field view showing large and well preserved echinoderms. b) Microphotograph showing echinoderms, numulites and micritized grains. c) Microphotograph showing well preserved coraline algae, micrite envelopes, drusy mosaic cement and quartz grains. d) Field view showing a layer of algae and branching bryozoans.

Cementation

The sediments of the An Nagaza Member exhibit four types of cementation. They are syntaxial overgrowth cement, isopachous cement, drusy mosaic cement and meniscus calcite cement.

***Syntaxial overgrowth cement*:** The syntaxial calcite overgrowths exist frequently around echinoderm debris (Figs. 4d and 5a). They exist in form of rims of variable thicknesses and of clean, coarse and bladed crystals with optical continuity with the grains (Evamy and Shearman, 1965).

***Isopachous cement*:** It appears as a rim of crystals of equal thickness on grains such as foraminifera (Fig. 10a). This cement exhibits a radial-fibrous fabric, and it may originally have been aragonite, details of the texture having been lost during inversion to calcite or during dissolution.

***Drusy mosaic cement*:** This type of calcite cement exhibits different crystal sizes, and it occurs as a drusy filling in many skeletal cavities of fossils, such as foraminifera tests, mollusk or bryozoans. The crystal size of the drusy mosaic cement increases towards the centre of cavities (Figs. 5d and 6a; 7b; 9c).

***Meniscus cement*:** Meniscus cement is irregularly distributed and it is precipitated in the vadoze zone as a result of water being held by capillarity between grains where it is concentrated. The crystals of this type of cement are fine to very fine mainly non-ferroan calcite at the grain contacts (Fig. 9c).

Compaction

The rocks of An Nagaza Member were likely subjected to only shallow burial. Mechanical compaction, i.e. grain to grain suture contact (Fig. 7a) and chemical compaction (Fig. 7d) are frequent and were the major diagenetic processes that existed in the shallow burial environment. The fractures within the carbonate and quartz grains probably resulted from physical compaction, during which they were filled by sparite or micrite respectively.

Dissolution

Dissolution and leaching features are present in all carbonates of the Al Khums Formation (An Nagaza Member). Dissolution resulted in the development of several types of porosity including interparticle or intergranular (see Fig. 4a), and moldic which mainly filled by later calcite cement (see Figs. 5d and 6a).

GEOCHEMISTRY RESULTS

Trace elements

Table 1 presents the results of the chemical analyses of the carbonates of samples selected from

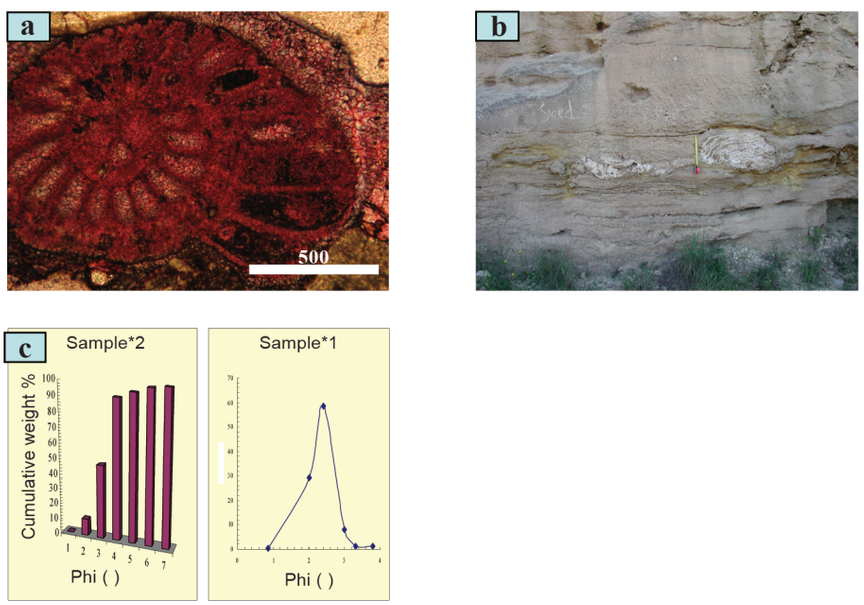

Fig. 10. a) Microphotograph of foraminifera from An Nagaza Member of the Al Khums Formation with probably isopachous cement. b) Field view showing different orientation of corals resulted from reworking. c) Cumulative curves illustrating sediments of beach environment.

Table 1. Chemical analyses (ppm) of selected samples from An Nagaza Member.

Sample no	Fe (ppm)	Mn (ppm)	Mg (ppm)	Sr (ppm)	Na (ppm)
SN1	2000	17	4000	300	31
SN2	1000	63	2000	82	57
SN3	8000	84	18000	70	86
SN4	9000	80	16000	100	95
SN5	7000	241	2000	58	59
SN6	2000	116	3000	100	93
SN7	2000	58	5000	100	69
SN7a	1000	60	1000	200	
SN8	4000	149	6000	54	62
SN9	1000	105	2000	300	79
SN10	4000	139	2000	500	175
SN11	1000	41	1000	100	59
SN12	1000	39	1000	28	55
SN14	2000	54	20000	31	24
SN15	2000	87	6000	100	31
SN16	2000	71	3000	100	58
SN17	2000	68	3000	67	72
SN18	2000	78	3000	81	66
SN19	1000	65	3000	82	79
SN20	3600	51	10000	66	43
SN21	2000	51	10000	76	44
SN22	1000	48	3000	90	52
SN23	2000	66	1000	100	44
SN24	2000	56	2000	91	38
SN25	2000	55	1000	100	11
SN26	3000	48	2000	100	6
SN27	2000	85	5000	89	28
SN28	3000	68	9000	100	27
SN29	5000	33	7000	200	180
SN30	3000	24	3000	200	21
SN31	7000	155	1000	100	3
SN32	1000	35	1000	100	9
SN33	1000	35	2000	100	80

An Nagaza Member of the Al Khums Formation. The variations in concentration of the elements analyzed reflect the diversity of their mineralogical compositions.

Fe contents in Lithofacies 1 range from 1000 to 9000ppm, with an average 4000ppm. The highest Fe content is concentrated at the base of Lithofacies 1, just above the sandstone bed where marl and clay increase. This may indicate that Fe concentration is mainly controlled by clay minerals. Fe concentration decreases significantly at the middle part of the Member (Lithofacies 2 and Lithofacies 3). It increases again towards the top of the Member (Lithofacies 4 and Lithofacies 5, Fig. 11).

Mn concentration increases from Lithofacies 1 (average 87ppm) to Lithofacies 2 (average 95ppm), but decreases towards the top of the Member (Fig. 11), averaging 71ppm and 62ppm in Lithofacies 3 and Lithofacies 5 respectively, with the lowest value observed in Lithofacies 4 (average 53ppm).

The lowest value of Mg was seen in Lithofacies 2 (average 2400ppm), whereas all other lithofacies exhibit more or less similar values.

Sr contents in all lithofacies are low with highest value recorded in Lithofacies 2 (average 196ppm). Generally, Sr contents increases from Lithofacies 1 (average 126ppm) to Lithofacies 2 (average 196ppm) and started to decrease towards Lithofacies 3 (average 77ppm), but increases again towards the top of the Member in Lithofacies 4 and Lithofacies 5 (89 and 127ppm in average respectively, Fig. 11).

Na concentrations in An Nagaza Member are low with highest value was observed in Lithofacies 2 (average 86ppm), whereas, the Na values in other lithofacies are 70ppm,55ppm, 34ppm and 50ppm in Lithofacies 1, 3, 4 and 5 respectively.

Isotopes

Oxygen Isotopes: Oxygen values for sediments of Lithofacies 1 (Table 2) vary from -3.9 to -7.5 ‰ (PDB). They are generally decreasing upward (Fig. 12), with maximum value recorded at the bottom of the lithofacies (-3.9‰), whereas the minimum being at top of the lithofacies (-7.5‰). The range narrows considerably at the middle of the lithofacies (-5.4 to -7.2‰). Oxygen isotopes do not vary greatly and exhibit narrow range in sediments designated as Lithofacies 2. They range from -5.2 to -7.8‰ (Fig. 12), with highest value observed at 22 metres (-5.2‰).

The variation in oxygen isotopes is very limited in Lithofacies 3. They range from -7.9 to -7.1‰), with a mean value of -7.5‰. Similarly, no great changes in the oxygen isotope values recorded in sediments of Lithofacies 4. They range from -7.4 to -5.9‰, with an average of -7.0‰. The range is quite wide of the oxygen isotope values in Lithofacies 5, from -7.3 to -2.2‰, with an average of -5.5‰. The highest values are observed at the middle of the lithofacies which correspond with decreasing $^{87}Sr/^{86}Sr$ (Fig. 12).

Carbon Isotopes: The $\delta^{13}C$- values of the lithofacies of the An Nagaza Member (Table 2) analyzed cover a wide range (-8.1 to 0.0‰), typical of carbonates formed in a near by continental environments, where decaying organic matter serves as a significant source of carbon for the dissolved inorganic carbon pool (Mayayo *et al*, 1996).

The lightest $\delta^{13}C$- values are found at the base of Lithofacies 1, with values from -8.1 to -3.3‰, and a mean of -4.7‰. Fig. 12, obviously shows that the

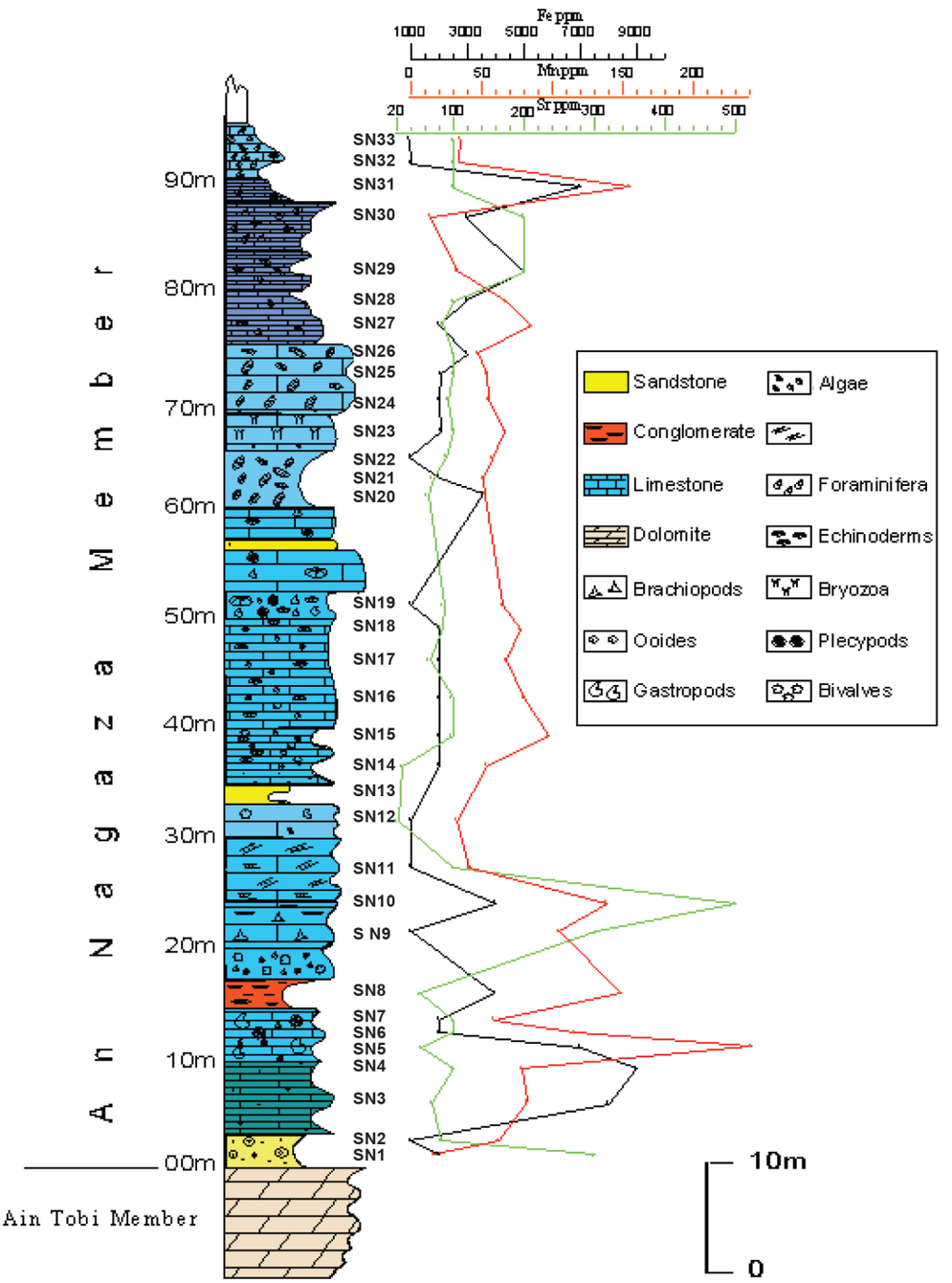

Fig. 11. Fe, Mn & Sr contents.

$\delta^{13}C$ getting heavier towards the top of the lithofacies. Carbon isotope values in sediments of Lithofacies 2 range from -5.6 to -2.3‰, with an average of (3.8‰). The highest value is observed at the bottom of the lithofacies. Generally, $\delta^{13}C$- values in Lithofacies 2 becoming lighter toward the top.

$\delta^{13}C$- values in both Lithofacies 3 and Lithofacies 4 cover narrow range (-3.6 to -1.1‰) and (-2.4 to 0.0‰) respectively. Lithofacies 3 shows slightly enriched carbon isotope values toward its top, on the other hand, $\delta^{13}C$- values in sediments of Lithofacies 4 are gradually depleted towards the top. Lithofacies 5 exhibits slightly wide range of $\delta^{13}C$- values (-6.9 to -2.1‰), with an average of -4.9‰. The $\delta^{13}C$- values of Lithofacies 5 getting lighter towards the top of the facies. Generally, $\delta^{13}C$- values are heavier towards the top of the member (Fig.12), with exception of Lithofacies 5, where the values

Table 2. Carbon and oxygen isotopic analyses of the selected samples from An Nagaza Member.

Sample no	$s^{13}C$	$s^{18}O$
SN1	-8.1	-3.9
SN2	-6.5	-6.3
SN3	-4.3	-7.2
SN4	-4.6	-6.9
SN5	-4.5	-7.5
SN6	-3.9	-5.4
SN7	-4.2	-7.2
SN7a	-3.3	-7.5
SN8	-2.4	-7.8
SN9	-2.3	-5.2
SN10	-3.7	-7.7
SN11	-4.9	-7.4
SN12	-5.6	-7.5
SN14	-3.6	-7.4
SN15	-3	-7.5
SN16	-2.3	-7.8
SN17	-1.5	-7.4
SN18	-2.2	-7.9
SN19	-1.1	-7.1
SN20	0	-5.9
SN21	-1.5	-7.4
SN22	-2.4	-6.9
SN23	-2.2	-7.1
SN24	-2.3	-6.8
SN25	-2	-6.8
SN26	-1.4	-6.8
SN27	-2.1	-7.3
SN28	-2.6	-5.8
SN29	-6.9	-2.9
SN30	-5.9	-2.2
SN31	-5.4	-7.2
SN32	-5.1	-7.1
SN33	-6.1	-6.3

are slightly lighter. It has been noticed that the highest values of $\delta^{13}C$ for most samples are opposite to the lowest values of $\delta^{18}O$ (Fig. 12).

Strontium Isotopes: Strontium isotope ratios presented in Table 3 ranges from 0.708438 to 0.708692. Corresponding ages have been calculated using the regression equations developed by Miller *et al*. (1991a) and Oslick *et al*. (1994). The former are based on the geomagnetic and polarity timescale of Berggren *et al*. (1985) whereas Oslick *et al*. (1994) also use the magnetic timescale of Cande and Kent (1992) to facilitate comparison with other studies. In each age calculation the measured $^{87}Sr/^{86}Sr$ ratios for the An Nagaza Member samples have been normalized to the relevant values obtained for the NBS 987 international isotope standard (0.710252 Miller *et al* and 0.710256 Oslick *et al*).

DISCUSSION AND INTERPRETATION

Environment of deposition: Desio (1971) mentioned the early Miocene transgression and the uplift of the area in the Late Miocene which resulted in the emergence of the area from the sea. Various fossils are indicative of shallow, neritic environment (Mann, 1975). The abundance of shallow water foraminifera as well as thick-shelled oyster, corals and the coralline algae with silisiclastic material suggest the shallow marine environment and were supplied into an outer neritic setting during Early Miocene.

Presence of horizons of limestone conglomerate and reworked fossils indicate periodic sea level rise and fall or times of increased wave action (Salem and Spreng, 1980). Furthermore, occurrence of ooids in the sediments of both Lithofacies 1 and Lithofacies 5 supporting the periodic sea level fluctuation and the mean temperature exceed $18^{O}C$. The grain supported nature of most of the lithofacies suggests

Table 3. Age determination (Ma) of the selected samples from An Nagaza Member.

Sample no	Sr87/Sr86	Age, Ma (Miller *et al*, 1991)	Age, Ma (Oslick *et al*, 1994)	
		BKF 1985	C & K 1992	BKF 1985
SN1	0.7086841	17.08	16.98	17.27
SN2	0.7086786	17.17	17.06	17.35
SN3	0.7085713	18.97	18.63	18.9
SN4	0.7085825	18.78	18.47	18.74
SN5	0.7085033	20.11	19.63	19.88
SN6	0.7086196	18.16	17.92	18.2
SN7	0.7086233	18.1	17.87	18.15
SN7a	0.7086233	18.1	17.87	18.15
SN8	0.7085522	19.29	18.91	19.18
SN9	0.7086809	17.13	17.03	17.32
SN10	0.7085939	18.59	18.3	18.57
SN11	0.7086689	17.33	17.2	17.49
SN12	0.7086634	17.43	17.28	17.57
SN14	0.7084986	20.19	19.7	19.95
SN15	0.7084989	20.19	19.69	19.95
SN16	0.7085038	20.1	19.62	19.88
SN17	0.7084877	20.37	19.86	20.11
SN18	0.7084557	20.91	20.32	20.57
SN19	0.7085054	20.08	19.6	19.85
SN20	0.7085315	19.64	19.21	19.47
SN21	0.7085203	19.83	19.38	19.64
SN22	0.7085455	19.4	19.01	19.27
SN23	0.7085639	19.1	18.74	19.01
SN24	0.7085681	19.03	18.68	18.95
SN25	0.7085608	19.15	18.79	19.05
SN26	0.7085303	19.66	19.23	19.49
SN27	0.7085566	19.22	18.85	19.11
SN28	0.7086432	17.77	17.58	17.86
SN29	0.7086562	17.55	17.39	17.67
SN30	0.7086497	17.66	17.48	17.77
SN31	0.7085687	19.02	18.67	18.94
SN32	0.7084377	21.21	20.59	20.83
SN33	0.708617	18.21	17.96	18.24

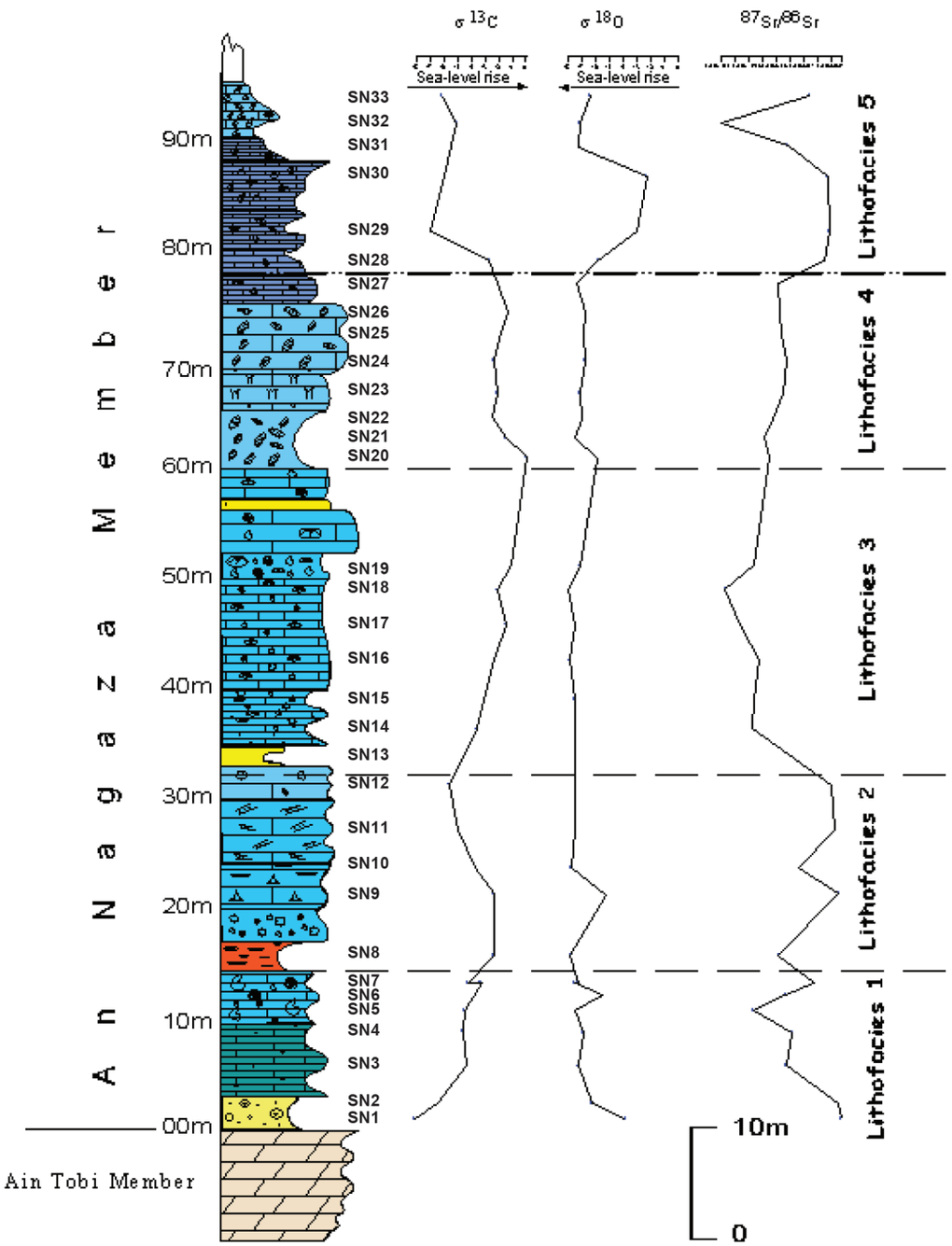

Fig. 12. Isotopes concentration of the An Nagaza Member (see Fig. 11. For symbols).

that the An Nagaza sediments were deposited in a medium to very high-energy marine environment. Vertical lithofacies variations and the presence of algae and branching bryozoans dominant lithofacies at the top of An Nagaza (Fig. 9d), suggest repeated shallowing upwards and elevated salinity. Corals and abundance of fossils indicate a warm water environment and probably normal salinity.

According to the results gained from the sieve analysis of two samples (standard deviation and skewness, Fig. 10c) the sandstones in the base of Lithofacies 1 seem to be deposited in a high-energy beach environment. The dominance of sandy grains in certain levels and less dominance in others of the An Nagaza sequence may also indicate fluctuation of sea level. Silisiclastic material is inferred to be recycled from older formations, perhaps exposed on nearby land areas, which were easily mobilized by marine coastal erosion during Miocene transgression.

Warm water, normal marine, moderate- to high-

energy, middle to outer neritic shelfal area, with reefoidal development, is postulated for An Nagaza sequence during Miocene. In summary, the complete succession of the An Nagaza sediments is interpreted as a transgressive sequence over the Cenomanian deposits, passing from marginal marine possibly to fully marine deposits.

***Diagenesis*:** The diagenetic features of the An Nagaza sediments of the Al Khums Formation seem to have occurred in different diagenetic environments. These are marine phreatic, mixed marine-meteoric and meteoric (Fig. 13).

***Micritization*:** Micritization is one of the early diagenetic processes and is inferred to have taken place in shallow marine environment. Micritization has preferentially affected shallow-water deposits and was most prevalent in low energy deposits. Micritization formed by combination of boring (by algae) and precipitation where the ambient waters are super saturated by calcium carbonate (Bathurst, 1966, 1975; Hook *et al*, 1984).

Micritization of skeletal grains in the An Nagaza sediments form micrite envelopes, which played an important role in preserving the fossil fragments during diagenesis. These envelopes have varying thicknesses and likely formed strictly within the marine phreatic environment near the sediment-water contact. The boundary between the micrite envelope and cement filled the molds and chambers of forams are irregular. This characteristic can be used to distinguish micrite envelopes from micrite coating around skeletal fragments. Also it can be taken as an evidence that this process occurred by blue-green algae (Adams *et al*, 1984).

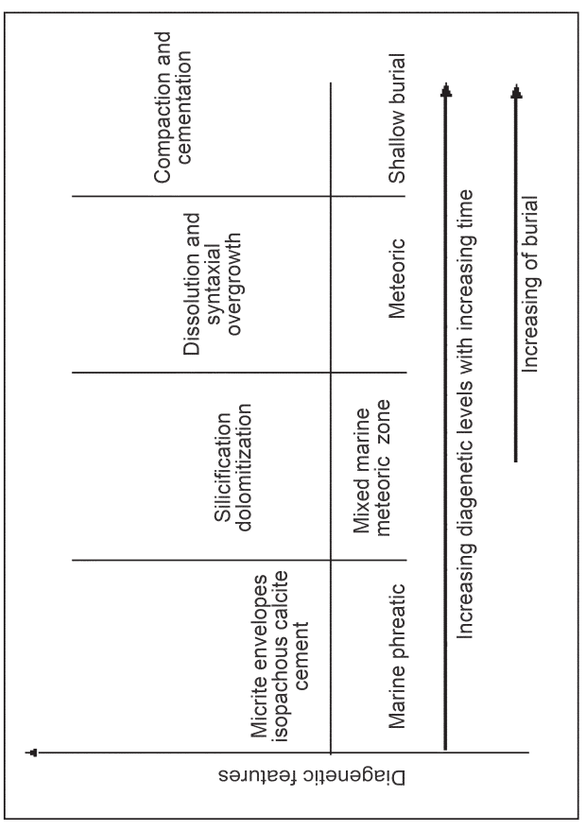

Fig. 13. Different diagenetic features during time and diagenetic environments detected in the An Nagaza Member.

***Compaction and Cementation*:** Lack of compaction in ancient carbonates is a sign of early cementation (Pray, 1960; and Steinen, 1978) and a shallow burial. Cementation in the An Nagaza deposits predates the mechanical compaction, as indicated by the random orientation of the components. In the uncemented beds, foraminifer's tests are broken and the components show a preferred orientation due to wave and current action, boring and mechanical compaction. Biogenic reworking would have destroyed any primary sedimentary structure within the beds. Chemical compaction through pressure dissolution is not able to rotate allochems such as corals (Bathurst, 1987; Figs. 6c and 10b); hence only mechanical compaction is suitable to explain this phenomenon. Pressure dissolution seems to play a minor role in the diagenesis of the examined sediments.

The diagenetic system in shallow-water carbonates with high initial aragonite content such as An Nagaza sequence is thought to be dominantly open (Bathurst, 1987 and Ricken, 1993). Relatively low aragonite content of the cemented (uncompacted) layers, in combination with the relatively high abundance of recrystallized allochems, shows that these layers were diagenetically altered. The onset of cementation in the carbonate layers is probably related to a formerly higher content of unstable carbonate components. In few examples, fracturing probably due to currents activity or mechanical compaction occurred after the development of syntaxial overgrowths on echinoid plates and postdates the formation of drusy non-ferroan spary calcite cement. These fractures remained open and unfilled by any cement, which taken as an evidence of later occurrences.

Syntaxial overgrowths form a minor cement phase restricted to echinoid plates or spins present in different facies of An Nagaza Member. Syntaxial overgrowths usually formed after Micritization (Fig.

13), and may either pre- or post-dates dissolution of aragonite.

The timing relationship of this cement phase relative to other diagenetic events suggests precipitation in a marine to meteoric or very shallow burial environment.

In the coral-rich facies non-ferroan isopachous cement is present around the bioclasts (Fig. 10a). This cement has often been overgrown by bladed or blocky cement, and may be replaced by equant, non-ferroan spary calcite, suggesting alteration of original aragonite. Isopachous cement is most likely represents early marine cement lost by dissolution, followed by recrystallization. This suggests the influence of meteoric water onto the sediments. The occurrence of recrystallization more than the leaching, is probably indicative of submarine precipitation, where nearly all of the pores were permanently filled with sea water. This conclusion is consistent with the suggestions of Land and Goreau (1970) and Marshal and Davis (1981).

Non-ferroan drusy calcite spar is the most common type of cement in the An Nagaza lithofacies, partially or completely occluding intergranular or biomoldic porosity (Figs. 5a and b and 6a). Drusy cements were precipitated after the formation of micrite envelopes. Where aragonite has been dissolved, drusy cements are often better developed between the bioclasts rather than within the biomolds. This suggests that dissolution coincide with the formation of drusy cements in the meteoric phreatic zone (Tucker and Wright, 1990). It is considered likely that calcite for the spar was derived from marine aragonitic bioclasts or cements. Equant, non-ferroan calcite spar is a minor cement phase replacing aragonitic bioclasts or micrite matrix in some sediments of the An Nagaza. It is inferred from the partial replacement nature of this cement that it formed in a shallow pre-burial or possibly meteoric environment.

Meniscus cement is composed of very small size crystals and occurred at the grain contacts. This type of cement is attributed to meteoric environment and it can forms from marine pore waters in the intertidal and supratidal zones as well as from meteoric waters.

***Trace Elements*:** Strontium concentration in diagenetic carbonates ranges from 20ppm to more than 10,000ppm (Land, 1973; Kimbell and Humphrey, 1994). Samples of the An Nagaza sediments have strontium concentration range from 28ppm to 500ppm (Table 1) typically reflects formation from a diagenetic fluid whose composition has been modified by the aragonite to calcite transformation.

Strontium concentration of a diagenetic carbonate samples such as An Nagaza may be a consequence of any combination of a variety of factors, including diagenetic fluid composition, temperature, biological effects, precipitation-rate, extent of recrystallization, type of mineral-solution reaction and crystal growth (Banner, 1995).

The low concentration of Sr and Mn in almost all samples of the An Nagaza Member could be attributed to the diagenetic effects produced by meteoric solutions which, in open systems, modify the chemical composition of carbonates in this way (Brand and Veizer, 1980; and Mayayo *et al*, 1996).

All samples of An Nagaza Member have high concentration of Fe (more than 1000ppm). This means that all samples are not exclusively carbonate and contain appreciable amounts of clay minerals and quartz grains.

Isotopes: The evaluation of the isotope values is somewhat complicated by the fact that bulk samples always contain different carbonate phases, organic carbon and components.

As $\sigma^{18}O$ values depend mainly on the temperature during precipitation (Morse and Mackenzie, 1991). Swart (2000) showed that the changes in the $\sigma^{18}O$ of pore waters along the Bahamas transect resulted from the recrystallization of metastable carbonates in the presence of a geothermal gradient.

The different fractionation factors of calcite and aragonite minerals would lead us to expect a shift towards lighter $\sigma^{18}O$ values in calcitic beds. However, the opposite is observed, the aragonitic beds are depleted in $\sigma^{18}O$. $\sigma^{18}O$ enrichment in the more cemented beds is consistent with a temperature decrease (Fig. 14) as indicated by Erez and Luz (1983).

It is evident that the $\sigma^{18}O$ values can be sensitive indicators of the degree of alteration of the initial metastable minerals comprising the matrix, which was probably formed from a mixture of aragonite and high-Mg calcite and the benthic fossils such as aragonitic mollusks and high-magnesium calcite forams (Shaaban, 2004).

The present $CaCO_3$ components (all are low-Mg calcite) represent the ultimate and product of the stabilization of the initial metastable $CaCO_3$ mineral phase. The close and depleted $\sigma^{18}O$ values of both rock matrix and benthic fossil particles indicate that fabric components probably suffered diagenetic

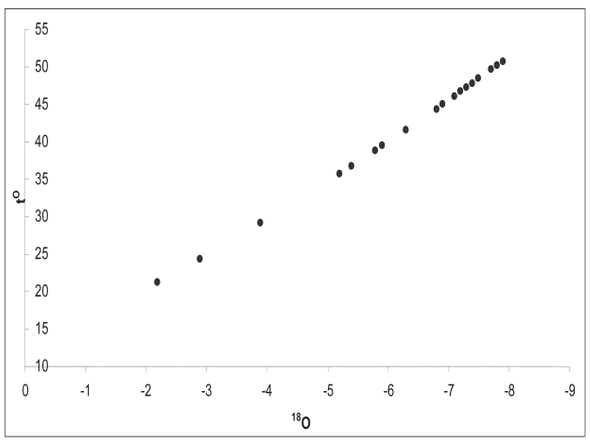

Fig. 14. Cross plot between temperature and oxygen isotope.

stabilization from freshwater dominated solutions undersaturated with respect to both high-Mg calcite and aragonite (Shaaban, 2004). This is true if we apply the following equation given by Hoefs (1973) on samples taken from An Nagaza sequence:

$Z = a(\sigma^{13}C+50) + b(\sigma^{18}O+50)$; where a= 2.048 and b= 0.498. Carbonate with a Z value above 120 would be classified as marine; those with a Z value below 120, as freshwater types. Most of the An Nagaza samples exhibit a Z values below 120, which suggest the strong influence of the freshwater solution.

Oxygen isotope data, compiled in Table 2, range from -2 to -7.9‰. These values are, possibly lower than expected from Miocene marine carbonates (Jacobs *et al*, 1996) and suggest that there may have been exchange with isotopically lighter meteoric water at one or more times in the past which has been approved by using the Hoefs (1973) equation. It may be argued that sample no. SN30 also suffered reworking. $\sigma^{18}O$ values of An Nagaza facies are significantly depleted (Table 2) compared to marine carbonate shells (Woo & Khim, 2006). Processes that can cause the depletion in $\sigma^{18}O$ for early diagenetic carbonates in marine silisiclastic deposits are summarized by Morad *et al* (1996); the influx of meteoric water, the oxidation of organic matter in sulphate-reduction zone, the interaction between seawater and sediments, the upwelling of hot fluids to near-surface, and the recrystallization or replacement of early carbonate cements during burial.

Neritic carbonates are enriched in ^{13}C compared to pelagic counterparts by 2-5‰ (Milliman, 1974). Hence, lithofacies (2, 3 and 4) with high neritic carbonate content display high $\sigma^{13}C$ values whereas; pelagic-rich lithofacies (1 and 5) have relatively low $\sigma^{13}C$ values.

The carbon isotope data range from 0.0 to -8.1‰. It is more difficult to assess the stability of the carbon isotopes because in marginal marine environment the carbon isotopes can be controlled by a number of factors. However, the relatively smooth change from low $\sigma^{13}C$ values in the bottom of the sequence (SN1 and SN2) to higher values, more typical of open marine water, and return to a low $\sigma^{13}C$ value in the top (SN33) may be an indication that a primary signal is preserved. This may be caused by a move from a restricted basin with high productivity, to more marine conditions, and back again (see the environment of deposition discussion section).

The Sr isotope composition of the An Nagaza samples of the Al Khums Formation corresponds to that of Early Miocene age. The calculated ages vary from 17 to 21 Ma, but not, as would be expected, in a systematic fashion which suggests that the carbonate samples may not be well preserved. The data scatter widely, suggesting mixing between a less radiogenic (marine) and more radiogenic meteoric components. Miller *et al* (1991a) related the changes of Sr isotopic in late Eocene to Miocene to glaciations and deglaciations of the Antarctica Craton. They explained the higher rate of change of $^{87}Sr/^{86}Sr$ during the early Miocene by an increase in the frequency of glaciations and the lower rate of change in the Middle Miocene by the development of a permanent ice cap in east Antarctica. Hodell *et al* (1991) and Raymo (1991) attributed the bulk of the Late Neogene $^{87}Sr/^{86}Sr$ increase to mountain uplift.

Sea Level Fluctuation: A $\sigma^{18}O$ decrease at the lower Miocene indicates that there was a large (more than 50m) glacioeustatic event (Miller, *et al*, 1991b). A $\sigma^{18}O$ decrease occurred in the middle of the Early Miocene suggest or may reflect glacioeustatic lowering of sea level and to the permanent ice sheet on Antarctica. Oslick *et al*, 1994 found that the increases in Sr isotopes are empirically linked to the oxygen isotope record. Oslick *et al* (1994) suggested that both mountain uplift and ice volume fluctuations contributed to the Neogene Sr isotopic signal. However, in the An Nagaza samples, the decrease of $\sigma^{18}O$ and increase of Sr isotopes could be attributed to the mountain uplift and glacioeustatic lowering of sea level.

Rises and falls of global sea-level, affecting the oxygen isotopic composition of sea-water. Thus, there should be a casual link between the record of $\sigma^{18}O$ in sea-water and the sedimentary record of sea-level fluctuations. Indeed, the composite isotope record of

the An Nagaza sequence does show several eustatic episodes at the time of deposition (Fig. 12) that are consistent with the geological record of ice-sheets evolution (Abreu and Anderson, 1998). In particular, negative excursions of the $\sigma^{18}O$ values should correspond to high sea-level stands and less negative or positive excursions to low sea-level stands. Furthermore, light $\sigma^{13}C$ observed in sediments deposited during low sea-level, while less negative or positive $\sigma^{13}C$ observed within sediments deposited during sea-level rise.

$\sigma^{18}O$ values record of the An Nagaza sequence are all negative indicating high sea-level stands during Early Miocene. At the beginning, sea transgressed over Cenomanian rocks, but its level was low as indicated by dominance of sandstone influx into the sequence, common shallow water fossils, depleted $\sigma^{13}C$ and less negative values of $\sigma^{18}O$, followed by relatively high stand for a short time (Fig. 12). This were succeeded by short lived regression of sea-water, followed again by sea-level rise for a considerable period of time as indicated by thick sequence of sediments rich in fossils of relatively deep marine (Fig. 12). At the end of the An Nagaza sequence, regression event took place followed by high sea-level stand.

In summary, the depletion of oxygen isotopes of the An Nagaza sediments were influenced by the following: 1- Temperature (Fig. 14), where less negative $\sigma^{18}O$ values consistent with decrease of temperature. 2- Diagenesis, including alteration of aragonite and high Mg-calcite to low Mg-calcite. 3- Lowering of sea-level during Miocene period. 4- Influx of meteoric water into the carbonate of the An Nagaza Member.

CONCLUSION

This study dealt with petrography and diagenesis of the An Nagaza Member of the Al Khums Formation in NW Libya. A total of 33 samples were collected for petrographic, stable isotopic and trace elements analysis. The samples of the An Nagaza were divided into five lithofacies; started with sediments resulted from transgression onto a Cretaceous surface of moderate relief. These sediments are of fossiliferous, reef-bearing with basal sand and limestone (Salem and Spreng, 1980). Lithofacies of the An Nagaza Member are mainly grain-supported and dominated by sandy packston to grainstone.

Various fossils present in the An Nagaza lithofacies are indicative of shallow, neritic environment. Furthermore, the abundance of silisiclastic material suggest the shallow marine environment and were supplied into an outer neritic setting during Early Miocene. The complete succession of the An Nagaza Member is interpreted as a transgressive sequence, passing from marginal marine to fully marine deposits.

The lithofacies of the An Nagaza sequence exposed to several different diagenetic events, which include both early and late stages. These lead to modification of their original textural and compositional characteristics. The diagenetic events occurred within this sequence including; micritization (formation of micrite envelopes and complete micritization), cementation (syntaxial overgrowth on echinoderms, isopachous, drusy mosaic and rarely meniscus), compaction and dissolution.

Micritization and formation of micrite envelopes are thought to be the first diagenetic event occurred within the An Nagaza sediments. They played an important role in preserving the fossil fragments during diagenesis. This process took place in the marine phreatic environment. The timing relationship of the syntaxial overgrowth cement phase relative to other diagenetic events suggests precipitation in a marine to meteoric or very shallow burial environment. Non-ferroan drusy calcite spar is the most common type of cement in the An Nagaza lithofacies. Drusy cements were precipitated after the formation of micrite envelopes and are often better developed where the aragonite has been dissolved. This suggests that dissolution coincide with the formation of drusy cements in the meteoric phreatic zone (Tucker & Wright, 1990).

The isotopes analysis of the An Nagaza samples shows that the oxygen isotope values range from -2.2‰ to -7.9‰ and carbon isotope values range from 0 to -8.2‰. Oxygen and carbon isotopes indicate that the sequence of the An Nagaza had exposed to sea-level fluctuation. Oxygen values are depleted; possibly because of exchange with isotopically lighter meteoric water at one or more times in the past. The smooth change from low $\sigma^{13}C$ values in the bottom of the sequence (SN1 and SN2) to higher values, more typical of open marine water, and a return to low $\sigma^{13}C$ value in the top (SN33) may be an indication that a primary signal is preserved. This may be caused by a move from a restricted basin with high productivity, to more marine conditions, and back again.

The Sr isotope composition of the An Nagaza samples of the Al Khums Formation corresponds to that of Early Miocene age. The calculated ages vary from 17 to 21 Ma. The changes of Sr isotopic in late Eocene to Miocene are related to glaciations and deglaciations of the Antarctica Craton (Miller *et al,* 1991a). Hodell *et al* (1991) and Raymo, 1991 attributed the bulk of the Late Neogene $^{87}Sr/^{86}Sr$ increase to mountain uplift. The Sr isotope increases of the An Nagaza samples may be related to both glaciations and deglaciations of the Antarctica Craton and to the mountain uplift.

Low Sr concentration in the An Nagaza sediments typically reflects formation from a diagenetic fluid whose composition has been modified by the aragonite to calcite transformation. This low concentration may be caused by extent of recrystallization and crystal growth. High Fe concentration of all samples indicates that they are not exclusively carbonate.

ACKNOWLEDGEMENTS

The authors would like to express their sincere thanks and appreciation to Dr Burima A. Belgasim, the former General Manager and all management of the Libyan Petroleum Institute (formerly, Petroleum Research Centre) for financing this work. Thanks go to the Dr. Mustafa J. Salem for guiding the field trips. We would also like to express our sincere thanks to Dr Mustafa Idris, the former General Manager of the Petroleum Research Centre for his help and cooperation during all stages of this work. We shall not forget to thank all our friends and colleges in the LPI, specially the Exploration and Exploitation Research Department staff for their help and support. Finally, we would like to thank the scientific committee members of the Exploration Researches, particularly its Chairman Prof. Ali Sbeta for his critical review and comments of the manuscript.

REFERENCES

Abreu, V. S. and Anderson, J. B., 1998. Glacial eustasy during the Cenozoic: sequence stratigraphic implications. *Bull. Am.Assoc.Petrol.Geol.,* ***82***, 1385-1400.

Adams, A. E., MacKenzie, W. S. and Guilford, C., 1984. *Atlas of Sedimentary Rocks Under the Microscope.* Halsted Press, John Wiley and Sons Inc, USA, 104p

Banner, J. L., 1995. Application of the trace element and isotope geochemistry of strontium to studies of carbonate diagenesis. *Sedimentology,* ***42***, 805-824.

Barr, F. T. and Weegar, A. A., 1972. *Stratigraphic Nomenclature of the Sirte Basin, Libya.* Publ. of the Petrol. Expl. Soc. of Libya, 179p.

Bathurst, R. G. C., 1966. Boring algae, micrite envelopes, and lithification of molluscan biosparites. *Geol. J.,* ***5***, 15-23.

Bathurst, R. G. C., 1975. Carbonate sediments and their diagenesis. *Development in Sedimentology,* ***12***, 658p.

Bathurst, R. G. C., 1983. Neomorphic spar versus cement in some Jurassic grainstones: significance for evaluation of porosity evolution and compaction. *J. Geol. Soc.,* ***14***, 229-237.

Bathurst, R. G. C., 1987. Diagenetically enhanced bedding in argillaceous platform limestones: stratified cementation and selective compaction. *Sedimentology,* ***34***, 749-778.

Berggren, W. A, Kent, D. V. and Flyn, J. J., 1985. Neogene geochronology and chronostratigraphy. *Mem. Geol. Soc. London,* ***10***, 211-259.

Brand, U. & Veizer, J., 1980. Chemical diagenesis of a multi-component carbonate system, 1. Trace elements. *J. Sediment. Petrol.,* ***50***, 1219-1236.

Cande, S. C. and Kent, D. V., 1992. A new geomagnetic polarity timescale for the Late Cretaceous and Cenozoic. *J. Geophysical Res.,* ***97***, 13917-13951.

Desio, A., 1971. Outlines and problems of the geomorphological evolution of Libya from the Tertiary to the present day. In: C. Gray, (ed.) *the Geology of Libya*, *First Symposium,* Faculty of Science, University of Libya, Tripoli, 11-36.

Dickson, J. A. D., 1965. A modified staining technique for carbonates in thin section. *Nature,* ***205***, p. 587

El-Waer, A. A., 1988. Miocene ostracoda from NW Libya. *J. Micropalaeontology,* ***7(1)***, 45-52.

El-Waer, A. A., 1991. Miocene ostracoda from the Al Khums Formation, NW Libya. In: M. J. Salem and M. N. Belaid (eds.), *The Geology of Libya,* ***V***., 1457-1482. Elsevier, Amsterdam.

Erez, J. and Luz, B., 1983. Experimental paleotemperature equation from planktonic foraminifera. *Geochim. Cosmochim. Acta,* ***47***, 1025-1031.

Evamy, B. D. and Shearman, D. J., 1965.The development of overgrowths from echinoderm fragments in limestones. *Sedimentology,* ***5***, 211-233.

Fatmi, A. N. and Sbeta, A. M., 1991. The significance of the occurrence of Abu Ghaylan and Kiklah formations east of Wadi Ghan, eastern Jabal Nafusah. In:. Salem, M. J., Sbeta, A. M. and Bakbak, M. R. (eds.) *The Geology of Libya*, ***VI***:,2227-2233.Elsevier,Amsterdam.

Floridia, G. B., 1939. Osservazioni sul Miocene del dintorni di Homs. *Boll. Soc. Geol. Ital.,* ***58***, 245-260.

Folk, R. L., 1965. Spectral subdivision of limestone types. In: W. E. Ham (ed.), Classification of Carbonate Rocks. *Mem. Am. Assoc. Petrol. Geol.,* ***1***, 62-84.

Hodell D. A., Mueller, P. A. and Garrido, J. R., 1991. Variations in the strontium isotope composition of seawater during the Neogene. *Geology,* ***19***, 24-27.

Hoefs, J., 1973. *Stable Isotope Geochemistry*. Springer-Verlag, New York: 208p.

Hook, J. E., Golubic, S. and Milliman, J. D., 1984. Micrite cement in microborings is not necessarily a shalow-water indicator. *J. Sed. Petrol.,* ***54***, 425-431.

Innocenti, F. and Pertusati, P., 1984. Sheet Al Aqaylah (NH 34-5), geological map of Libya, scale 1: 250,000, with explanatory booklet. *Industrial Research Centre*, Tripoli.

Jacobs, E., Weissert, H. and Shields, G., 1996. The monterey event in the Mediterranean: a record from the shelf sediments of Malta. *Palaeoceanography, **11***, 717-728.

Kimbell, T. N. and Humphrey, J. D., 1994. Geochemistry and crystal morphology of aragonite cements of mixing-zone origin, Barbadose, West Indies. *J. Sed. Res., **A64***, 604-614.

Land, L. S., 1973. Holocene meteoric dolomitization of Pleistocene limestones, north Jamaica. *Sedimentology, **20***, 411-424.

Land, L. S. and Goreau, U. F. (1970). Submarine lithification of Jamaican reefs. *J. Sed. Petrol., **40***, 457-462.

Mann, K., 1975. Sheet Al Khums (NI 33-14), geological map of Libya, scale 1: 250,000,with explanatory booklet. *Industrial Research Centre*, Tripol, Libya.

Marshal, F. F. and Davis, P. J., 1981. Submarine lithification on windward reef slopes: Capricom-Bunker group, southern great barrier reef. *J. Sed. Petrol., **51***, 953-960.

Mayayo, M. J., Bauluz, B, Lopez-Galindo, A.and Gonzalez-Lopez, J. M., 1996. Mineralogy and geochemistry of the carbonates in the Calatayud Basin (Zaragoza, Spain). *Chemical Geology, **130***, 123-136.

Milliman, J. D., 1974. *Marine Carbonates*. Springer-Verlag, Berlin: 375p.

Mijalkovic, N. (1977). Sheet Al Qaddahiyah (NH 33-3), Geological map of Libya, scale 1: 250,000,with explanatory booklet. *Industrial Research Centre*, Tripol, Libya.

Miller, K. G., Feigenson, M. D., Wright, J. D. and Clement, B. M., 1991a. Miocene isotope reference section, Deep Sea Drilling Project Site 608: An evaluation of isotope and biostratigraphic resolution. *Palaeoceanography, **6***, 33-52.

Miller, K. G., Wright, J. D. and Fairbanks, R. G., 1991b. Unlocking the ice-house. *J. Geophys. Res., **96***, 6829-6848.

Morad, S. De Ros, L. F. and Al-Aasm, I. S., 1996. Origin of low $\sigma^{18}O$, precompactional ferroan carbonates in the marine Sto Formation (Middle Jurassic), offshore NW Norway. *Mari. Petolr. Geolg., **13***, 263-276.

Morse, J. W. and MacKenzie, F. T., 1991. Influence of solution chemistry and reaction kinetics on $CaCO_3$ transport in subsurface environments. *Geol. Soc. Amer., Abstr. with program, **23***, A318.

Oslick, J. S., Miller, K. G., Feigenson, M. D. and Wright, J. D., 1994. Oligocene – Miocene strontium isotopes: stratigraphic revisions and correlations to an inferred glacioeustatic record. *Palaeoceanography, **9***, 427-443.

Pray, L. C., 1960. Compaction in calcilutites (abstract), *Bull. Geol. Soc. Am., **71***, p. 1946.

Raymo, M. E., 1991. Geochemical evidence supporting T. C. Chamberlin's theory of glaciation. *Geology, **19***, 344-347.

Ricken, W., 1993. *Sedimentation as a Three-component System.* Lecture Notes in Earth Science, **51**. Springer, Berlin: 211p.

Salem, M. J. and Spreng, A. C., 1980. Middle Miocene stratigraphy, Al Khums area, northwestern Libya. In: M. J. Salem, and M. T. Busrewil (edts.), *Second Symposium on the Geology of Libya. **I,*** 97-116, London Academic Press.

Shaaban, M. N., 2004. Diagenesis of the lower Eocene Thebes Formation, Gebel Rewagen area, eastern desert, Egypt. *Sedim. Geol., **165(1-2,*** 53-65.

Sherif, K., 1991. Biostratigraphy of the Miocene in Al Khums area, northwest Libya. In: M. J. Salem and M. N. Belaid (eds.), *The Geology of Libya, **V***., 1421-1456, Elsevier, Amsterdam.

Steinen, R. P., 1978. On the diagenesis of lime mud: scanning electron microscopic observations on sub-surface material from Barbados. *J. Sed. Petrol., **48***, 1139-1147.

Swart, P. K. (2000). The Oxygen Isotopic Composition of Interstitial Waters: Evidence for Fluid Flow and Recrystallization in the Margin of Great Bahama Bank. In: P. K. Swart, G. P. Eberli, M. J. Malone, J. F. Sarg (eds.), *Proc. ODP Sci., Results, **166***, 91-98.

Tucker, M. E. & Wright, V. P., 1990. *Carbonate Sedimentology*. Blackwell Scientific Publications, Oxford: 482p.

Woo, K. S. & Khim, B., 2006. Stable oxygen and carbon isotopes of carbonate concretions of the Miocene Yeonil Group in the Pohang Basin, Korea: types of concretions and formation condition. *Sediment. Geol., **183(1-2)***, 15-30.

Zivanovich, M., 1977. Sheet Bani Walid (NH 33-2), *Geological map of Libya, scale 1: 250,000, with explanatory booklet.* Industrial Research Centre, Tripoli, Libya.